Quantitative Analysis of Anterior Discectomy and Fusion Spine using Fractal Dimension Analysis

Alejandro Venable-Croft[1], Walker Welch[2,3], Kate Watkins[2,3], Garret Burks, PhD[2], Johnathan J. Carmouche, MD, MBA [2,3], Caitlyn Collins PhD[1]
[1]Virginia Tech, Biomedical Engineering, Blacksburg Virginia, USA, [2]Virginia Tech-Carillion School of Medicine, Roanoke, Virginia, USA, [3]Department of Orthopaedics and Neurosciences, Carillion Clinic, Roanoke, Virginia, USA
venablecrofta@vt.edu

Disclosures: Alejandro Venable-Croft (N), Walker Welch (N), Kate Watkins (N), Garret Burks (N), Jonathan J. Carmouche (N), Caitlyn J. Collins (N)

Introduction: Anterior Cervical Discectomy and Fusion (ACDF) is a common surgical procedure used to treat spinal pathologies such as degenerative disc disease, cervical spondylosis, and spinal instability. More than 700,000 operations are conducted yearly, representing 60% of all cervical spine surgeries in the US. The postoperative assessments of spinal arthrodesis, or fusion, typically involve radiological examinations – starting with plain radiographs – as the standard of care for monitoring fusion progression. Plain radiography, while readily available, is susceptible to inconsistent patient positioning and lower resolution than advanced 3D imaging, which make it difficult to assess images quickly and consistently. Further, x-ray evaluations rely on either qualitative interpretation of radiolucency or metrics such as the Interspinous Distance and Cobb Angle which do not directly assess the fusion mass between two surgical vertebrae. A reliable, quantitative approach capable of capturing fusion dynamics longitudinally and directly from the interbody region could offer clinicians earlier and more consistent insight into bone healing and non-union risk. The purpose of this study is to characterize the temporal trajectory of spinal fusion utilizing a quantitative, image-based metric to directly assess bone growth within the post-surgical spine.

METHODS: 339 longitudinal lateral plain x-rays (LXR) from patients undergoing ACDF were identified for an IRB-approved study on early diagnostic tools for pseudarthrosis. Eligible patient radiographs were selected based on the following criteria: 1) primary fusion surgery, 2) presence of a C5-6 fusion 3) imaging from at least 4 follow-up visits. After filtering for these criteria, 24 patients were eligible for this analysis and longitudinal LXR were transformed using rigid image registration. Three (ROIs) representing the anterior region (A), posterior region (P), and midpoints (M) were identified in each image (**Fig. 1**). The radius of the ROI was defined as the distance between the superior and inferior vertebrae. The same radius was used for each of the 3 ROIs, within a given patient and timepoint. Fractal dimension analysis, namely the Hurst and Variable Orientation Transforms, HOT and VOT, respectively, was used to detect changes in bone growth over time within the surgical site. Each analysis generated two summary metrics: the Hurst coefficient (H), which reflects the degree of organization of bone, and the rescaled range (RS), which represents the overall variability in bone intensity (**Fig. 2**). These transforms have previously been used to detect heterogeneity and progression of knee osteoarthritis using plain radiographs; in this study they were used to quantify changes in bone structure within the ROI at each time point. Normality and equal variance tests were performed using the Shapiro-Wilke and Brown-Forsythe tests, respectively. Results were analyzed using a mixed-effect repeated measure ANOVA, with visit as a fixed effect and patient as a random effect; post-hoc Tukey tests were performed to analyze group differences (SAS JMP Pro 18). P-values < 0.05 were considered significant.

RESULTS: 24 patients (mean age: 56±12.8 years, 52% female) were included in this study. Significant differences in the RS values were observed for both HOT and VOT methods; however, H values were not significantly different for either. Mixed effects modeling demonstrated a clear peak in fusion-related values centered at Visit 2 (**Fig. 3A and Table 1**). While post-hoc Tukey tests did not identify differences between this peak and adjacent visits, the effect relative to baseline was consistently larger than at all-other time points: .431 ± .067 ($p<.0001$) and .285 ± .060 ($p<.0001$) for HOT and VOT respectively.

DISCUSSION: A peak in distributions was found at visit 2 for both H and RS, using both HOT and VOT methods, corresponding to the 3-week ± 2.4 weeks follow-up timepoint. This may indicate a period of maximal remodeling activity during which new bone begins to permeate consistently throughout the ROI, aligning with early bone remodeling behavior. From this point, it may be possible to predict patient fusion trajectories. Closer inspection revealed that a single patient with confirmed C5-6 pseudarthrosis had lower values for both methods across the analyzed time frame, remaining below the 25th percentile throughout analysis. These decreased RS and H values were accompanied by a lower high-intensity to low-intensity pixel coverage ratio within the ROIs, suggesting a lower rate of bone growth over time compared to other patients. This methodology's ability to detect differences across the full follow-up period is limited by the small cohort size and visit time variability and the resulting sensitivity to patient level variation. Furthermore, differentiation between healthy and pseudarthritic patients remains constrained for the same reason. Despite limitations, this work successfully characterized fusion dynamics quantitatively during the first interval of standard-of-care imaging using LXR-image processing.

SIGNIFICANCE/CLINICAL RELEVANCE: The image-based fractal dimension analyses that were deployed in this study successfully assessed direct interbody fusion, qualitatively, in the post-operative spine, reducing interobserver variations and dependence on qualitative clinical assessments.

IMAGES AND TABLES:

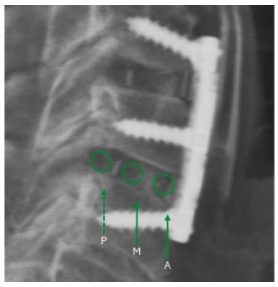

Fig. 1: LXR ROIs for A) Anterior, B) Midline, C) Posterior sites.

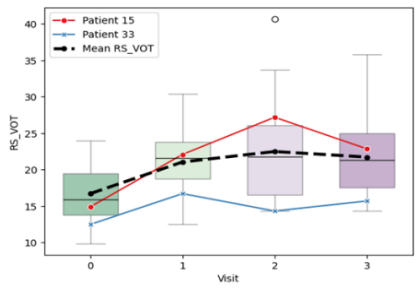

Fig. 2: Mean curve data for Rescaled Range (n=24) across visits 0, 1, 2, 3.

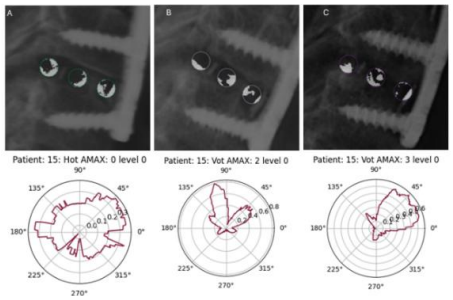

Figure 3: ROIs with threshold set for bone (top) and rose plots of VOT data from sample patient for visits A) 0, B) 2, and C) 3.

Table 1: Summary of Reported Rescaled Range difference for HOT and VOT methodologies (n=24) with visit wise comparisons

	Visit Comparison	Difference	t Ratio	p		Visit Comparison	Difference	t Ratio	p
HOT	**0-1**	**-0.356±0.067**	**-5.29**	**<.0001**	VOT	**0-1**	**-0.24±0.060**	**-3.98**	**0.0009**
	0-2	**-0.431±0.067**	**-6.41**	**<.0001**		**0-2**	**-0.285±0.060**	**-4.72**	**<.0001**
	0-3	**-0.384±0.067**	**-5.71**	**<.0001**		**0-3**	**-0.261±0.060**	**-4.33**	**0.0003**
	1-2	-0.075±0.067	-1.12	0.6796		1-2	-0.045±0.060	-0.74	0.8813
	1-3	-0.028±0.067	-0.41	0.9758		1-3	-0.021±0.060	-0.35	0.9848
	2-3	0.047±0.067	0.7	0.8952		2-3	0.023±0.060	0.39	0.9804